Improved Dynamic Performance and Hierarchical Energy Management of Microgrids With Energy Routing

Jameel Ahmad, Muhammad Tahir, *Member, IEEE*, and Sudip K. Mazumder, *Fellow, IEEE*

***Abstract*—In this paper, a hierarchical distributed energy management of multimicrogrids (MMGs) with energy routing is proposed. Existing control strategies for power sharing, transient performance, and economic-emission dispatch in microgrids with distributed generators (DGs) fall short in providing good dynamic performance. To address this issue, a hierarchical distributed optimization is proposed by using top–down approach, which decomposes original economic-emission dispatch of MMG scenario into individual microgrid (MG) and energy routing subproblems. Distributed electric vehicle charging, intermittent photovoltaic source, and battery energy storage system are incorporated in the optimization model. Using multiagent system model for DG, a dynamic performance controller (DPC) is proposed for each MG to achieve improved performance during transients. Convergence of optimization algorithm is proved using Lyapunov theory. Performance evaluation results show that the proposed DPC for economic-emission dispatch improves system performance significantly during either load or generator switching.**

***Index Terms*—Distributed generation, dynamic performance, energy router, economic-emission dispatch, multiagent system (MAS).**

I. Introduction

ENVIRONMENTAL concerns and anticipated global energy crisis have accelerated efforts to increase reliability and improve economic efficiency of power systems. As a result, more and more renewable energy sources are being integrated, resulting in reduced carbon emissions. Particularly, the use of photovoltaic (PV) systems, battery energy storage systems (BESS), wind turbines, and fuel cells, etc., has emerged as an attractive solution to meet energy demands of a small community in a distributed manner giving birth to community MGs. These MGs are becoming integral part of today's power system infrastructure giving birth to cluster of MGs or multimicrogrids (MMGs) [1]–[4] for distributed energy management.

Manuscript received May 25, 2018; revised September 1, 2018; accepted October 8, 2018. The work of Prof. S.K. Mazumder was supported by the U.S. NSF Award 1644874. Paper no. TII-18-1304. *(Corresponding author: Muhammad Tahir.)*

J. Ahmad is with the Department of Electrical Engineering, University of Management and Technology, Lahore 54700, Pakistan, and also with the Department of Electrical Engineering, University of Engineering and Technology, Lahore, Lahore 54890, Pakistan (e-mail: jameel.ahmad@umt.edu.pk).

M. Tahir is with the Department of Electrical Engineering and Al-Khwarizmi Institute of Computer Science, University of Engineering and Technology, Lahore, Lahore 54890, Pakistan (e-mail: mtahir@uet.edu.pk).

S. K. Mazumder is with the Department of Electrical and Computer Engineering, University of Illinois at Chicago, Chicago IL 60607 USA (e-mail: mazumder@uic.edu).

Color versions of one or more of the figures in this paper are available online at http://ieeexplore.ieee.org.

Digital Object Identifier 10.1109/TII.2018.2877739

An MG typically is a low-voltage power distribution network comprising of different distributed generators (DGs), controllable electric loads, and energy storage devices. MGs can operate both in islanded as well as grid-connected modes [5]. A DG refers to a small power generation unit, which usually has capacity of few megawatt. The DGs in an MG can communicate with each other through a suitably designed communication network for optimal power sharing, energy state monitoring, and distributed control. In recent years, the increased penetration of these MGs has posed additional requirements and challenges for power system operators, such as dynamic economic dispatch (DED), efficient control of transients in case of source-load fluctuations, and power quality among many others.

Economic dispatch is commonly defined as the process of determining the optimal generation cost and meeting load demands along with operational constraints. Different solutions have been proposed for ED, such as DED, real-time ED (RTED), to name a few. The authors in [6] have formulated DED problem as a two stage primal-dual problem using Lagrangian relaxation. A possible extension is distributed DED that can be implemented by using multiagent system (MAS) architecture [7]. A relaxation of economic dispatch (RED) problem using distributed Laplacian based first-order dynamics is discussed in [8]. A key limitation of the above-mentioned ED solution approaches is inferior dynamic performance in case of load or source transients.

Conventionally, the ED problem for traditional power systems is performed on a slower time scale (see Fig. 1) independent of automatic generation control (AGC) that is performed at faster time scale. In case of an MG, load demand uncertainties as well as the number of renewable sources are on the rise, which result in frequent source-load transients as well as larger power fluctuations. This demands for faster ED to not only improve the economical efficiency of the system but also to bridge the time gap between ED and AGC [9]. The authors in [10] have proposed to integrate AGC and ED for real-time optimization, where ED in the feedback loop is activated at discrete time instants.

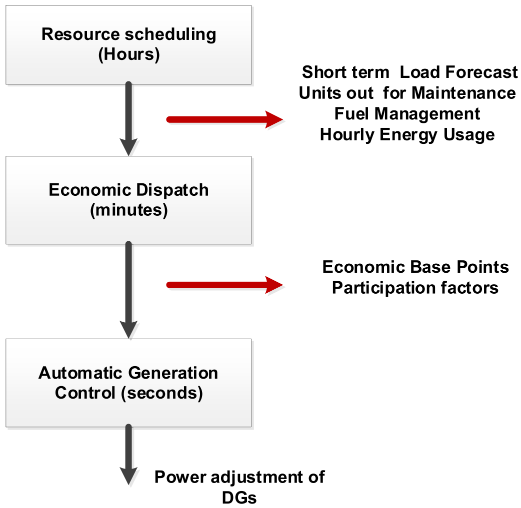

Fig. 1. Time scale of resource scheduler, ED and AGC.

However, this solution suffers from poor dynamic performance due to ED activation at slower time scale.

DED that can respond to fast fluctuations in the generation as well as load demand [11], for interconnected MGs [12], is therefore highly desirable to optimize energy management, control energy flow among MGs and ensure supply–demand balance [13]. To meet these objectives, conventional primal-dual algorithm based ED is extended in this paper to an augmented Lagrangian based dynamic control allowing the implementation of a *dynamic performance controller* (DPC). A hierarchical design involving multiagent system (MAS) based MG control architecture and energy router based inter-MG power flow control, is proposed for energy management in MMG scenario. Traditionally, multiagent-based architecture converges to average consensus [14], which effectively leads to equal load sharing among DGs in an MG, which may lead to poor economic efficiency. To address this limitation, a relaxation of consensus constraint is introduced. The proposed approach is equally useful for grid connected as well as islanded modes of operation. However, it is more effective for islanded mode of operation, since transients can be more pronounced in that case. Key contributions of this paper are summarized below.

1) Optimization problem formulation as hierarchical distributed optimization for MMGs using augmented Lagrangian based control algorithm for single MG to improve dynamic performance.
2) Multiagent communication system architecture for MG and energy router for controlling inter-MG power flow for MMGs.
3) Optimal power sharing among DGs integrated with renewable energy sources and distributed charging loads, such as electric vehicle (EV) along with economic-emission dispatch.

The paper is organized as follows. In Section II-A, MMG system architecture is outlined. This section also provides communication framework using multiagents. Optimization problem formulation for hierarchical distributed optimization for MMGs with energy routers is presented in Section III. The problem is further decomposed into multiple subproblems for simultaneous optimization. An augmented Lagrangian based optimized control is provided for an MG with renewable and nonrenewable energy sources in Section IV. Performance evaluation results are provided in Section V, and conclusion in Section VI.

II. System Model

The key components of an MMG system architecture include the MG itself along with the devices used to create connectivity among multiple MGs. Next, we discuss these two components to elaborate the system model.

A. Single MG System Architecture

Each MG has certain number of DGs connected to it, which are responsible for economic power sharing to meet the load demand. In the present study, it is assumed that each MG has traditional DGs, renewable energy sources e.g., PV panels along with BESS. In addition, controllable loads are connected to each MG, whose values can be configured.

MG employs hierarchical control strategy and uses primary control to maintain operating voltage and frequency. Secondary control provides active and reactive power control, which is also termed as AGC, while tertiary control is used to implement ED. To minimize generation cost, different DGs are operated at optimal power generation point. It is assumed that the controllers installed with the renewable sources are responsible for delivering energy to the system, but they do not take part in the ED. Rather the DGs with only nonrenewable energy sources participate in the ED to improve the system performance during transients.

For distributed implementation of ED in each MG, we select a set of N DGs and correspondingly define set $\mathcal{N} = \{1, 2, \ldots, N\}$. Each DG$_i$ has an associated group of neighboring DGs, which are denoted by the set $N_i \subset \mathcal{N}$. The set N_i includes all of the DGs that have direct communication link with DG$_i$. The communication links between any pair of DGs are assumed to be bidirectional. This scenario can be modeled using an undirected graph $G_d = \{N, E\}$, where E represents the set of all communication links that exist among the DG pairs.

Now, for the above-mentioned graph G, define an adjacency matrix $A = A(G_d)$, with $A \in \mathbb{R}^{N\times N}$. Each element $a_{l,m} \in A$, is set equal to 1, when the link $(l, m) \in E$, that is the corresponding communication link exists between DG$_l$ and DG$_m$ and is set to 0 otherwise. If $a_{l,m} = 1$, then DG$_l$ and DG$_m$ are considered to be adjacent to each other. Now considering the communication view point, the degree d_l of a generator DG$_l$ is defined as the total number of DGs that are adjacent to it and can be evaluated as $d_l = \sum_{m\in N_l, m\neq l} a_{l,m}, \forall l$. Define $D \in R^{N\times N}$ as the diagonal matrix with corresponding entries $d_l, l \in \{1, 2, \ldots, N\}$ and is termed as the degree-matrix for the graph G. Now using the adjacency and degree matrices, one can define the graph Laplacian matrix, M as $M = D - A$. The Laplacian matrix M has all of its row sums equal to zero, i.e., $M\mathbf{1} = 0$, where $\mathbf{1}$ represents an all ones vector. For proper communication among distributed agents, it is assumed that the delay to transmit the parametric

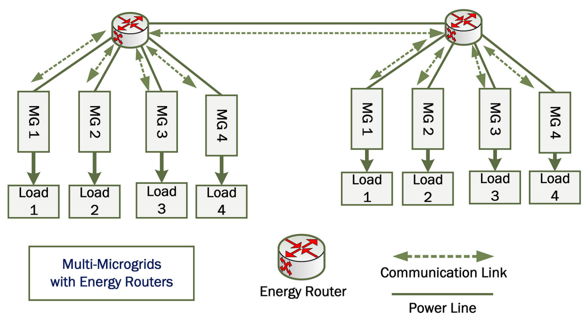

Fig. 2. MGs with energy routing.

information among the neighboring DGs is much lower than the interval required by the controller to update its output.

B. MMG Architecture Using Energy Router

An energy router operates at MG level and monitors, the power produced and consumed in each MG and can communicate with the DGs of the MGs that are connected to it. Energy routers are also responsible for power exchange as well as direction control of power flow between interconnected MGs.

In a typical cluster of MGs as shown in Fig. 2, all the MGs are interconnected through energy routers via their power lines and communication interfaces. The MG DGs can communicate at different levels. At lower level of the hierarchy DGs communicate with other neighboring DGs within the MG, thus forming the MAS architecture of the MG. At the higher level some of the DGs in an MG communicate to energy routers, making power exchange among multiple MGs possible.

Clustered MGs with DG are prone to power fluctuations due to uncertainty, variability and forecast errors in renewable power generation. Energy routers are being deployed to compensate for shortage of power by injecting power from one MG to another MG to meet its load demand by using energy routing. A hierarchical structure integrating DGs in MGs with energy routers is shown in Fig. 2, where MG to MG power exchange via two energy routers is depicted.

III. Problem Formulation for MMG Architecture With Energy Routers

In this section, a multiobjective optimization problem is formulated for network of MGs connected using energy routers. First, component of the multiobjective cost function is for economic-emission dispatch and is defined for each MG. Second, cost function accounts for PV power intermittency. Third, cost component captures the price of energy exchange between any pair of connect MGs.

A. Economic-Emission Cost

The ED problem is formulated as an optimization problem with an objective function to minimize total generation cost of DGs. For this purpose, a quadratic cost function C_i is defined as below

$$\sum_i C_i(p_i) = \sum_i \alpha_i p_i^2 + \beta_i p_i + \gamma_i, \quad \forall i. \tag{1}$$

In (1), $p_i \in \mathbf{p}, \ \mathbf{p} \in \mathbb{R}^N$ represent the power delivered from generator i, while α_i, β_i, and γ_i are the generation cost coefficients of the ith generator. The economic-emission dispatch problem can be modeled by incorporating cost of reducing pollutant emissions (e.g., reducing emissions of CO_2, NOx, and SOx). Among the three pollutants, NOx, CO_2, and SOx, considered in literature, CO_2 is the most dominant. Pollutant emission cost, $E_i(p_i)$, follows quadratic cost [15], [16] and is given by

$$\sum_i E_i(p_i) = \sum_i a_i p_i^2 + b_i p_i + c_i, \quad \forall i \tag{2}$$

where a, b, and c are pollutant emission cost coefficients. Since (1) and (2) are both quadratic functions, these can be combined into one function by adding (1) and (2) making it an economic-emission cost function as given below

$$\sum_i D_i(p_i) = \sum_i A_i p_i^2 + B_i p_i + C_i, \quad \forall i \tag{3}$$

where $A_i = a_i + \alpha_i$, $B_i = b_i + \beta_i$, and $C_i = c_i + \gamma_i$ are economic-emission cost coefficients.

B. Supply–Demand Balance and Power Exchange Between MGs

Conventional thermal generators and PV generators are considered in this analysis. Now, define the following parameters.

$p_{i,m}^{(G)}$:	Power generated by ith DG in mth MG,
$p_m^{(\mathrm{PV})}$:	PV power from mth MG,
$p_m^{(B)}$:	Battery power from mth MG,
$p_{k,m}$:	Power flowing from kth MG to mth MG and governed by energy router,
$L_{dm} + L_{dm}^{(\mathrm{EV})}$:	Total load as sum of conventional load, L_{dm} and distributed EV load, $L_{dm}^{(\mathrm{EV})}$ in mth MG,
$\sum_k p_{k,m} - \sum_j p_{m,j}$:	Difference of total power received by mth MG from k MGs and total power delivered by mth MG to j MGs,

The power supply–demand balance can be written as

$$\sum_i p_{i,m}^{(G)} + p_m^{(\mathrm{PV})} + p_m^{(B)} + \left(\sum_k p_{k,m} - \sum_j p_{m,j}\right) = L_{dm} + L_{dm}^{(\mathrm{EV})}, \quad \forall m \tag{4}$$

Therein, an MG can inject power into another MG, if it has surplus power. It is assumed that main grid will play a role of passive constant grid and will not participate in optimization. All interconnected MGs will exchange power and energy router will ensure this power sharing.

C. Cost of PV Power Intermittency

Distributed renewable energy resources may generate power fluctuation because of uncertain generation behavior. It is

TABLE I
BESS PARAMETERS

BESS	η_p	η_c	η_{loss}	Min. output(kW)	Max. output(kW)
1	0.15	.01	0.1	-50	50
2	.2	.01	.12	-50	50
3	.3	.0.01	.1	-50	50

Q3

assumed that each MG will have PV power sources, whose power output variation will also affect power sharing among interconnected MGs. To account for this fact, an intermittency cost component is introduced in the objective function in (8a). The operational and maintenance costs of PV are minimal and are ignored. Cost function for lumped PV power, $p_m^{(\mathrm{PV})}$ in mth MG can be modeled as

$$C_m\left(p_m^{(\mathrm{PV})}\right) = m_1 p_m^{(\mathrm{PV})} + \epsilon_m \exp\left(m_2 - p_m^{(\mathrm{PV})}\right) \quad \forall m \quad (5)$$

where $m_1 > 0$, $m_2 > 0$, and $\epsilon_m > 0$. The first term in (5) denotes the direct operating cost, while the second term denotes the penalty on curtailment of PV power generation [17].

D. Operational Cost of BESS

A BESS is included and batteries are charged when buying price is cheaper and vice versa. Batteries are operational with reasonable depth of discharge and battery operational cost, B_m for lumped battery power, $p_m^{(B)}$ in mth MG is modeled as [18],

$$\sum_m B_m\left(p_m^{(B)}\right) = \sum_m \eta_p p_m + \eta_c\,|p_m| + \eta_{\mathrm{loss}} p_m^2, \quad \forall m \quad (6)$$

where η_p and η_c are electricity price and battery cost parameter, respectively, and η_{loss} is the loss cost parameter (see Table I).

E. Energy Router and Cost of Power Exchange

In smart grid scenario, consumers can share and exchange energy-like information in the internet. The energy router is an emerging device concept [19]–[21] that is based on advanced power electronic techniques for control of energy exchange among MGs. Energy router in MMG scenario aims at increasing energy exchange efficiency and optimizes dispatch of energy between MGs.

We have modeled cost of power exchange between MGs connected through energy router as a quadratic cost function. Effectively, the quadratic cost function discourages power exchange between any pair of MGs that are connected through an energy router. This enables the system to keep efficiency loss to minimum by reducing conversion losses incurred by the power converter. In addition, it also reduces line losses by reducing power flow between generators and loads that are far apart. Now, the cost of power transfer, F from kth MG to mth MG can be conveniently defined as

$$F = u_m p_{k,m}^2 \quad (7)$$

where u_m is cost coefficient for power transfer between MGs and $p_{k,m}$ is power flowing from kth MG to mth. The value of u_m is taken as 1.

F. Optimization Problem Formulation for MMG

There is an underlying tradeoff among the conflicting objectives of reducing cost of pollutant emissions, reducing generation cost of thermal generators, reducing operational and curtailment cost of PV and cost of power transfer between MGs with the help of energy router. The multiobjective economic-emission dispatch problem with PV penetration and power exchange between MGs can now be formulated for all m MGs, based on above details as follows.

$$\min \sum_m \left\{ \sum_i D_i\left(p_{i,m}^{(G)}\right) + C_m\left(p_m^{(\mathrm{PV})}\right) + B_m\left(p_m^{(B)}\right) + \sum_k F_m\left(p_{k,m}\right) \right\} \quad (8a)$$

$$\text{subject to} \quad \mathbf{M_m p_m} + \delta_m \geq 0, \quad (8b)$$

$$\sum_i p_{i,m}^{(G)} + p_m^{(\mathrm{PV})} + p_m^{(B)} + \left(\sum_k p_{k,m} - \sum_j p_{m,j}\right) = L_{dm} + L_{dm}^{(\mathrm{EV})}, \quad (8c)$$

$$p_{i,m}^{\min} \leq p_{i,m}^{(G)} \leq p_{i,m}^{\max} \quad (8d)$$

where $\mathbf{M_m}$ is the Laplacian matrix of DGs in mth MG and $\mathbf{p_m}$ is a vector of powers generated from all DGs in mth MG. The first inequality constraint in (8b) is termed as the relaxed consensus constraint with relaxation coefficient δ_m. When $\delta_m = 0$, $\mathbf{M_m p_m} = 0$, then this constraint becomes the consensus constraint. The second equality constraint in (8c) is supply–demand balance. The third constraint in (8d) is about upper and lower power limits of DGs in an MG. A partial Lagrangian function, $\mathcal{L}_a$ for MMG case can now be derived from (8a) and is given by

$$\min \left(\mathcal{L}_a\left(\mathbf{p_{i,m}^{(G)}}, \mathbf{p_{k,m}}, \mathbf{p_m^{(PV)}}, \mathbf{p_m^{(B)}}, \lambda\right)\right) = \sum_m \left\{ \sum_i D_i\left(p_{i,m}^{(G)}\right) + B_m\left(p_m^{(B)}\right) + C_m\left(p_m^{(\mathrm{PV})}\right) + \sum_k F_m\left(p_{k,m}\right) \right\} + \sum_m \lambda_m \left\{ L_{dm} + L_{dm}^{(\mathrm{EV})} - \sum_i p_{i,m}^{(G)} - p_m^{(\mathrm{PV})} - p_m^{(B)} - \left(\sum_k p_{k,m} - \sum_j p_{m,j}\right) \right\}\Bigg)$$

$$\text{subject to} \quad \mathbf{M_m p_m} + \delta_m \geq 0, \quad p_{i,m}^{\min} \leq p_{i,m}^{(G)} \leq p_{i,m}^{\max} \quad (9)$$

Problem in (9) can be decomposed into two subproblems, namely MG subproblem and energy router subproblem that can be solved independently.

1) MG Subproblem: This problem is solved for each MG separately. The objective in this case is to solve (10) and generate optimal powers from each DG i.e., $p^{*}_{i,m}$, operate PV power sources at $p_m^{*(\text{PV})}$ and operate batteries with optimal charging/discharging powers at $p_m^{*(B)}$. Each MG subproblem involves solving a multiagent problem of its own and can be considered a second level of distributed optimization.

$$\min \ \sum_i D_i\left(p_{i,m}^{(G)}\right) + C_m\left(p_m^{(\text{PV})}\right) + B_m\left(p_m^{(B)}\right) + \lambda_m\left\{L_{dm} + L_{dm}^{(\text{EV})} - \sum_i p_{i,m}^{(G)} - p_m^{(PV)} - p_m^{(B)}\right\}$$
$$\text{subject to } \ \mathbf{M_m p_m} + \delta_m \geq 0, \ \ p_{i,m}^{\min} \leq p_{i,m}^{(G)} \leq p_{i,m}^{\max} \tag{10}$$

2) Energy Router Subproblem:

$$\min \ F_m\left(p_{k,m}\right) - \lambda_m\left\{\sum_k p_{k,m} - \sum_j p_{m,j}\right\} \tag{11}$$

3) Dual Problem:

$$\max \ g(\lambda) = \pounds\left(\mathbf{p^{*(G)}_{i,m}}, \mathbf{p^{*}_{k,m}}, \mathbf{p_m^{*(PV)}}, \mathbf{p_m^{*(B)}}, \lambda\right) \tag{12}$$

G. Distributed Implementation

Each MG is considered as a node in higher level power network with a tree-like structure. In this scheme, the energy is routed from the MG with surplus power generation capacity to the MG, which has power shortage to supply its internal loads. The shortage of power can happen due to unavailability or intermittency of one of its DGs. An MG can receive power from another MG with lower cost of production. Each MG problem involves a multiagent problem and is solved independently by each MG. MG subproblem (10) solves for $p_{i,m}^{*(G)}$, $p_m^{*(\text{PV})}$, $p_m^{*(B)}$ and sends this information to dual problem (12) and it sends back optimal incremental cost λ_m^*. Similarly, energy router problem (11) computes optimal $p_{k,m}^*$ and sends this information to dual problem (12) and it sends back optimal incremental cost λ_m^* to router problem (11). Effectively, this problem decomposition implements a hierarchical distributed optimization. The advantage of this scheme is its scalability and ease of implementation. Many more clusters of MG and energy routers can be incorporated in a tree-like structure without much computational overhead.

IV. Dynamics and Optimized Control of MG Subproblem

For single MG, the optimization problem (8a) reduces to MG subproblem (10). The previously used notation for MG e.g., using subscript m can be dropped conveniently simplifying notation and therfore, in (10), $\mathbf{M} \in \mathbb{R}^{N\times N}$ and $\delta \in \mathbb{R}^N$. L_d denotes the load demand in each MG. The first equality constraint is supply–demand balance. The second equality constraint in (10) is termed as the relaxed consensus constraint with relaxation coefficient δ. When $\delta = 0$, $\mathbf{Mp} = 0$, then this constraint becomes the consensus constraint. By allowing $\delta \geq 0$ and correspondingly $\mathbf{Mp} + \delta \geq 0$, consensus constraint is relaxed, which in turn provides the flexibility to reduce the overall generation cost. The last set of constraints in (10) are individual generator minimum and maximum power generation limits. In (10), $p_m^{(\text{PV})}$ is power output from PV panels, $p_m^{(B)}$ is power output from battery unit, $L_d^{(\text{EV})}$ is a distributed charging load due to EVs, which also affects system transients. The problem in (10) can be solved using the Lagrangian duality. In conventional ED problem, a constrained optimization problem is formulated using Lagrange multiplier theory. As shown later in this section, this conventional approach is equivalent to integral-based control, which results in poor dynamic performance. To improve the dynamic performance, DPC-based optimized ED solution approach is proposed. Due to the inherent integral control action, the dynamic performance of optimized power generation may not be satisfactory. The Lagrangian, $\pounds_b$ for the optimization problem (10) is defined as given below

$$\begin{aligned}
\pounds_b\left(\mathbf{p}, \mathbf{p_m^{(PV)}}, \mathbf{p_m^{(B)}}, \lambda, \mathbf{\Phi}\right) &= \sum_i D_i(p_i) + C_m\left(p_m^{(\text{PV})}\right) \\
&+ B_m(p_m^{(B)}) + \left\{\lambda\left\{L_d + L_d^{(\text{EV})} - \sum_i p_i - p_m^{(\text{PV})} - p_m^{(B)}\right\}\right. \\
&\left. + \Phi^t[\mathbf{Mp} + \delta]\right\} - \sum_i \left\{\theta_i^{\min}(p_i - p_i^{\min})\right. \\
&\left. + \theta_i^{\max}(p_i^{\max} - p_i)\right\}, \forall i
\end{aligned} \tag{13}$$

In (13), λ and Φ are the Lagrange multipliers (or dual variables) for equality constraints in (10) associated with the load–supply balance and consensus, respectively, and $\theta_i^{\min}$ and $\theta_i^{\max}$ are Lagrange multipliers for inequality constraint in (10) for each DG. Using (13), next the primal-dual dynamics is developed. The optimal conditions for the optimization problem in (10) can be achieved by taking partial derivatives of $\pounds_b$ with respect to each decision variable and setting each equation in (14) equal to zero. Without considering the generator inequality constraints, a set of first-order dynamic equations for single MG can be derived as follows.

$$\begin{aligned}
\dot{p}_i &= k_{p_i}\left\{D_i'(p_i) - \lambda + \Phi^t M_i\right\}, \ \ \forall i \\
\dot{p}_{pv} &= k_{p_{pv}} C_m'\left(p_m^{(\text{PV})}\right), \quad \dot{p}_B = k_{p_B} B_m'\left(p_m^{(B)}\right) \\
\dot{\lambda}_i &= k_{\lambda_i}\left\{L_d + L_d^{(\text{EV})} - \sum_i p_i - p_m^{(\text{PV})} - p_m^{(B)}\right\}^+, \forall i \\
\dot{\phi}_i &= k_{\phi_i}\left\{[\mathbf{Mp}]_i + \delta_i\right\}^+, \ \ \forall i
\end{aligned} \tag{14}$$

In (14), M_i represents the ith column of $\mathbf{M}$, $[\mathbf{Mp}]_i$ denotes the ith element of vector $\mathbf{Mp}$ and $\phi_i \in \Phi$. The parameters k_{p_i}, $k_{p_{pv}}$, k_{p_B}, k_{λ_i}, and k_{ϕ_i} are the step size scaling coefficients, while the notation $\{z\}^+$ in (14) is defined as $\max\{0, z\}$. It should be realized that the generator power updates, based on the dynamics given by the first expression in (14), are subject to the minimum and maximum power constraints. Let $u_i = \Phi^t M_i - \lambda$ is the control action. Using the expression for λ from (14) and substituting to the control action u_i, the system dynamic equations can be rewritten as

$$\begin{aligned} \dot{p}_i &= k_{p_i}\left\{D_i'(p_i) + u_i\right\}, \quad \forall i \\ \dot{p}_{pv} &= k_{p_{pv}} C_m'\left(p_m^{(\mathrm{PV})}\right), \quad \dot{p}_B = k_{p_B} B_m'\left(p_m^{(B)}\right) \\ u_i &= \left\{\Phi^t M_i - k_{\lambda_i}\int_0^t \left\{L_d + L_d^{(\mathrm{EV})}\right.\right. \\ &\quad \left.\left. - \sum_i p_i(\tau) - p_m^{(\mathrm{PV})}(\tau) - p_m^{(B)}(\tau)\right\}^+ d\tau\right\}, \quad \forall i \\ \phi_i &= k_{\phi_i}\int_0^t \left\{[\mathbf{Mp}(\tau)]_i + \delta_i\right\}^+ d\tau, \quad \forall i \end{aligned} \tag{15}$$

The auxiliary variable u_i in (15) is in fact the control law, which effectively implements an integral control to achieve desired economic-emission dispatch. To improve the dynamic performance during power transients due to any variations in load demand, a distributed DPCbased solution is developed. This is achieved by modifying the system dynamics in (15), to construct an augmented Lagrangian function $\mathcal{L}_c$ from (13) and is given by

$$\begin{aligned} &\mathcal{L}_c\left(\mathbf{p}, \mathbf{p_m^{(PV)}}, \mathbf{p_m^{(B)}}\lambda, \Phi, \tilde{\mathbf{p}}\right) \\ &= \sum_i (D_i(p_i)) + C_m\left(p_m^{(\mathrm{PV})}\right) + B_m(p_m^{(B)}) \\ &\quad + k_1^{(i)}\left\{\lambda\left(L_d + L_d^{(\mathrm{EV})} - \sum_i p_i - p_m^{(\mathrm{PV})}\right) - p_m^{(B)})\right. \\ &\quad \left. + \Phi^t[\mathbf{Mp} + \delta]\right\} + \left(k_2^{(i)}\right)/2\left\{\sum_i (p_i - \tilde{p}_i)^2\right\} \\ &\quad + \left(k_3^{(i)}\right)/2(L_d + L_d^{(\mathrm{EV})} - \sum_i p_i - p_m^{(PV)} - p_m^{(B)})^2 \end{aligned} \tag{16}$$

In (16), $k_1^{(i)}$, $k_2^{(i)}$, and $k_3^{(i)}$ are integral, derivative, and proportional gains, respectively, and $\tilde{p}_i$ is an auxiliary state variable. The integral term in (16) is same as in (13), while two more terms are introduced in augmented Lagrangian. The functionality of these terms will be verified later in this section. It is worth mentioning that the last term with gain $k_3^{(i)}$, in augmented Lagrangian, is introduced using only supply–demand balance constraint to respond to any variations in the load. Using augmented Lagrangian in (16) the updated primal dual dynamics becomes

$$\begin{aligned} \dot{p}_i &= k_{p_i}\left(D_i'(p_i) + u_i\right), \ \forall i, \quad \dot{\tilde{p}}_i = \tilde{k}_{p_i}(p_i - \tilde{p}_i), \ \forall i \\ \dot{p}_{pv} &= k_{p_{pv}} C_m'\left(p_m^{(\mathrm{PV})}\right), \quad \dot{p}_B = k_{p_B} B_m'\left(p_m^{(B)}\right) \\ \dot{\lambda}_i &= k_{\lambda_i}\left\{L_d + L_d^{(\mathrm{EV})} - \sum_i p_i - p_m^{(\mathrm{PV})} - p_m^{(B)}\right\}^+, \forall i \\ \dot{\phi}_i &= k_{\phi_i}\left\{[\mathbf{Mp}]_i + \delta_i\right\}^+, \quad \forall i \end{aligned} \tag{17}$$

where *control law* u_i is given by

$$u_i = -k_1^{(i)}[\lambda - \Phi^t M_i] + k_2^{(i)}(p_i - \tilde{p}_i) - k_3^{(i)}\psi(\dot{\lambda}), \quad \forall i. \tag{18}$$

The first expression in (17) represents the power system dynamics for economic-emission dispatch and the associated controller, u_i. k_{p_i} is a gain term associated with generators first-order power dynamics. The second expression is responsible for PV power variation due to irradiance and temperature.The third expression is responsible for battery power. The fourth expression effectively implements the derivative control as discussed later, while the fifth and sixth expressions in (17) are the same dual variable updates obtained in (14). The control u_i in (18) implements a novel dynamic controller called DPC, where $\psi(.)$ is a linear functional mapping. The first term, in (18), is the integral control action as discussed previously. The last term implements a sort of proportional control action. This can be verified using a simple linear functional mapping as $\psi(\dot{\lambda}) = \dot{\lambda}$. The $\dot{\lambda}$ is proportional to p_i, as verified using the third expression of (17) and results in proportional control action. The structure of the proposed DPC is, in fact, a modified version of a basic PID controller. The second term in (18) implements the derivative control action. The second term, $k_2^{(i)}(p_i - \tilde{p}_i)$, in (18) converges to zero at equilibrium and equivalently, the auxiliary variable $\tilde{p}_i$ converges to p_i, $\forall i$. This term is responsible for implementing derivative control action in variable p_i, as verified below. For this purpose, applying Laplace transformation to $\dot{\tilde{p}}_i = \tilde{k}_{p_i}(p_i - \tilde{p}_i)$, results in

$$\tilde{p}_i(s) = \frac{\tilde{k}_{p_i}}{s + \tilde{k}_{p_i}} p_i(s). \tag{19}$$

Substituting $\tilde{p}_i(s)$ from (19) to the expression $k_2^{(i)}(p_i - \tilde{p}_i)$, it becomes $\frac{k_2^{(i)}}{s+\tilde{k}_{p_i}} s p_i(s)$, which implements derivative control in p_i, while the coefficient $\frac{k_2^{(i)}}{s+\tilde{k}_{p_i}}$ implements low pass filtering. Choosing a large value of gain parameter $\tilde{k}_{p_i}$ increases the bandwidth of derivative control.

A. Distributed Consensus Algorithm

Our algorithm is distributed in the sense that no leader or master nodes are needed, while all the nodes (generators) conduct local computation and communicate with their neighbors. The solution to the optimal control problem given in (17) can be found in an iterative procedure by exchanging the primal and dual variables among the DG agents for their computations. By choosing small enough positive values for k_{p_i}, $k_{p_{pv}}$, k_{p_B}, $\tilde{k}_{p_i}$, k_{λ_i}, and k_{ϕ_i} in (17), the update (17) would converge to the optimal point of the problem [22]. However, using (17) requires each node having access to certain global information of the MG's load demand and power generation of all DGs and values for PV generation. To make the algorithm (17) distributed, instead of using global information, DG agents are allowed to use local value and share this information with their neighboring agents and try to achieve consensus.

Each DG agent gathers information locally and communicate with other neighboring DG agents in the MG. The Laplacian matrix is responsible for connectivity among DGs. The information among the DGs is exchanged using wireless link (e.g., WiFi or Wireless Broadband) based communication interface. Agents communicate at the application level and any agent communication language (ACL) can be employed as the application layer protocol. For instance, FIPA-ACL [23] one possible ACL that can be used for this purpose.

B. Proof of Convergence

The convergence of DPC-based DED can be analyzed using Lyapunov stability theory. For that purpose, let us define $\bar{\mathbf{p}} = [\mathbf{p}^t\ \tilde{\mathbf{p}}^t\ \mathbf{p}_{\mathbf{m}}^{(\mathbf{PV})}\ \mathbf{p}_{\mathbf{m}}^{(\mathbf{B})}]^t$. It is straightforward to verify that the augmented Lagrangian $\mathcal{L}_c(\mathbf{p}, \mathbf{p}_{\mathbf{m}}^{(\mathbf{PV})}, \mathbf{p}_{\mathbf{m}}^{(\mathbf{B})}, \lambda, \Phi, \tilde{\mathbf{p}})$ in (16) is a convex function of $\bar{\mathbf{p}}$, while it is concave in λ and Φ. In addition, we minimize $\mathcal{L}_c(\bar{\mathbf{p}}, \lambda, \Phi)$ with respect to $\bar{\mathbf{p}}$, while it is maximized for λ and Φ. Using this fact and combining it with first-order convexity condition [24], we obtain following expression.

$$\dot{\bar{p}}_i = -k_{\bar{p}_i} \frac{\partial \mathcal{L}_c}{\partial \bar{p}_i},\quad \dot{\lambda} = k_{\lambda} \frac{\partial \mathcal{L}_c}{\partial \lambda},\quad \dot{\phi}_i = k_{\phi_i} \frac{\partial \mathcal{L}_c}{\partial \phi_i}, \forall i. \tag{20}$$

In (20), $k_{\bar{p}_i}$ can be either k_{p_i} or $\tilde{k}_{p_i}$. Now using the second-order condition for convexity, we obtain

$$\frac{\partial^2 \mathcal{L}_c}{\partial \bar{p}_i^2} \geq 0,\quad \frac{\partial^2 \mathcal{L}_c}{\partial \lambda^2} \leq 0,\quad \frac{\partial^2 \mathcal{L}_c}{\partial \phi_i^2} \leq 0\ \ \forall i. \tag{21}$$

For stability analysis, we use Lyapunov theory. Specifically, we use the following candidate Lyapunov function to prove the stability of the proposed dynamic controller.

$$V(\bar{p}, \lambda, \Phi) = \begin{bmatrix} g(\bar{p}) & g(\lambda) & g(\Phi) \end{bmatrix} Q \begin{bmatrix} g(\bar{p}) \\ g(\lambda) \\ g(\Phi) \end{bmatrix}. \tag{22}$$

The Lyapunov function, in (22), is based on Krasovskii's method [25], where $g(.)$ is a functional mapping of state dynamics as defined later in this section. For the candidate function in (22), the matrix Q is required to be positive definite i.e., $Q > 0$ and $Q^t = Q$. A possible choice for Q, which fulfills the above mentioned requirements is given by

$$Q = \frac{1}{2} \begin{bmatrix} \Pi^{-1} & 0 & 0 \\ 0 & k_{\lambda}^{-1} & 0 \\ 0 & 0 & \Gamma^{-1} \end{bmatrix}. \tag{23}$$

In (23), Π and Γ are diagonal matrices with appropriate dimensions, where k_{ϕ_i} are diagonal entries of matrix Γ, while k_{p_i} and $\tilde{k}_{p_i}$ are diagonal entries of matrix Π. Next time derivative of Lyapunov function $V(\bar{p}, \lambda, \Phi)$, results in

$$\dot{V}(\bar{p}, \lambda, \Phi) = \begin{bmatrix} \dot{\bar{p}}\ \dot{\lambda}\ \dot{\Phi} \end{bmatrix} \begin{bmatrix} \frac{\partial g(\bar{p})}{\partial \bar{p}} & \frac{\partial g(\lambda)}{\partial \bar{p}} & \frac{\partial g(\Phi)}{\partial \bar{p}} \\ \frac{\partial g(\bar{p})}{\partial \lambda} & \frac{\partial g(\lambda)}{\partial \lambda} & \frac{\partial g(\Phi)}{\partial \lambda} \\ \frac{\partial g(\bar{p})}{\partial \Phi} & \frac{\partial g(\lambda)}{\partial \Phi} & \frac{\partial g(\Phi)}{\partial \Phi} \end{bmatrix}$$

$$Q + Q \begin{bmatrix} \frac{\partial g(\bar{p})}{\partial \bar{p}} & \frac{\partial g(\bar{p})}{\partial \lambda} & \frac{\partial g(\bar{p})}{\partial \Phi} \\ \frac{\partial g(\lambda)}{\partial \bar{p}} & \frac{\partial g(\lambda)}{\partial \lambda} & \frac{\partial g(\lambda)}{\partial \Phi} \\ \frac{\partial g(\Phi)}{\partial \bar{p}} & \frac{\partial g(\Phi)}{\partial \lambda} & \frac{\partial g(\Phi)}{\partial \Phi} \end{bmatrix} \begin{bmatrix} \dot{\bar{p}} \\ \dot{\lambda} \\ \dot{\Phi} \end{bmatrix}. \tag{24}$$

Now let us define $g(\bar{p}) = \dot{\bar{p}}, g(\lambda) = \dot{\lambda}, g(\Phi) = \dot{\Phi}$. Combining this, with first- and second-order convexity conditions given in (20) and (21), results in the following expression.

$$\begin{bmatrix} \frac{\partial g(\bar{p})}{\partial \bar{p}} & \frac{\partial g(\bar{p})}{\partial \lambda} & \frac{\partial g(\bar{p})}{\partial \Phi} \\ \frac{\partial g(\lambda)}{\partial \bar{p}} & \frac{\partial g(\lambda)}{\partial \lambda} & \frac{\partial g(\lambda)}{\partial \Phi} \\ \frac{\partial g(\Phi)}{\partial \bar{p}} & \frac{\partial g(\Phi)}{\partial \lambda} & \frac{\partial g(\Phi)}{\partial \Phi} \end{bmatrix} = \frac{1}{2} \begin{bmatrix} \frac{-\partial^2 \mathcal{L}_c}{\partial \bar{p}^2} & \frac{-\partial^2 \mathcal{L}_c}{\partial \lambda \partial \bar{p}} & \frac{-\partial^2 \mathcal{L}_c}{\partial \lambda \partial \bar{p}} \\ \frac{\partial^2 \mathcal{L}_c}{\partial \bar{p} \partial \lambda} & \frac{\partial^2 \mathcal{L}_c}{\partial \lambda^2} & \frac{\partial^2 \mathcal{L}_c}{\partial \Phi \partial \lambda} \\ \frac{\partial^2 \mathcal{L}_c}{\partial \bar{p} \partial \Phi} & \frac{\partial^2 \mathcal{L}_c}{\partial \lambda \partial \Phi} & \frac{\partial^2 \mathcal{L}_c}{\partial \Phi^2} \end{bmatrix}. \tag{25}$$

Substituting (25) to (24), we obtain

$$\dot{V}(\bar{p}, \lambda, \Phi) = \begin{bmatrix} \dot{\bar{p}} & \dot{\lambda} & \dot{\Phi} \end{bmatrix}$$

$$\begin{bmatrix} \frac{-\partial^2 \mathcal{L}_c}{\partial \bar{p}^2} & \frac{-\partial^2 \mathcal{L}_c}{\partial \lambda \partial \bar{p}} & \frac{-\partial^2 \mathcal{L}_c}{\partial \Phi \partial \bar{p}} \\ \frac{\partial^2 \mathcal{L}_c}{\partial \bar{p} \partial \lambda} & \frac{\partial^2 \mathcal{L}_c}{\partial \lambda^2} & \frac{\partial^2 \mathcal{L}_c}{\partial \Phi \partial \lambda} \\ \frac{\partial^2 \mathcal{L}_c}{\partial \bar{p} \partial \Phi} & \frac{\partial^2 \mathcal{L}_c}{\partial \lambda \partial \Phi} & \frac{\partial^2 \mathcal{L}_c}{\partial \Phi^2} \end{bmatrix} \begin{bmatrix} \dot{\bar{p}} \\ \dot{\lambda} \\ \dot{\Phi} \end{bmatrix}. \tag{26}$$

The stability of DPC is established by using the second-order condition for convexity in (26). In particular, we get $\dot{V}(\bar{p}, \lambda, \Phi) \leq 0$ by using the LaSalle's invariance principle [25].

V. Performance Results

A. MG1: Single MG

For the optimized power flow control from DG, a network of four DGs [26] is studied. Each DG consists of a controller, an energy source, and a power converter. The proposed DPC algorithm is applicable for both grid connected as well as islanded mode of operation. Connectivity among four DGs in MG1 is illustrated in Fig. 3. For given connectivity graph among DGs in MG1, corresponding Laplacian matrix M_1 for MG1 is given by

$$M_1 = \begin{bmatrix} 1 & -1 & 0 & 0 \\ -1 & 3 & -1 & -1 \\ 0 & -1 & 2 & -1 \\ 0 & -1 & -1 & 2 \end{bmatrix}. \tag{27}$$

Maximum power generation limits for four generators are tabulated in Table II. Generator minimum power limit, $p_i^{\min}$ is set to 0.5 MW for all generators. It is assumed that generators are conventional thermal power units with cost parameters given in Table II , which are obtained from [27]. Emission cost parameters in Table II are derived from [15]. A total power demand of 4 MW is assumed. Information among the DGs is exchanged using an IEEE 802.15.4 based communication interface, which provides data rate of 250 Kbps. Step size scaling coefficients

TABLE II
GENERATION, EMISSION COST COEFFICIENTS, AND SYSTEM PARAMETERS

	Parameter.	DG1	DG2	DG3	DG4
MG1	α	1×10^{-5}	1.5×10^{-5}	2.5×10^{-5}	2×10^{-5}
	β	5×10^{-3}	2×10^{-3}	2.5×10^{-3}	4×10^{-3}
	γ	0.10	0.15	0.09	0.075
	a	4.091×10^{-3}	2.543×10^{-3}	4.258×10^{-3}	5.426×10^{-3}
	b	-5.554×10^{-3}	-6.047×10^{-3}	-5.094×10^{-3}	-3.550×10^{-3}
	c	6.490×10^{-3}	5.638×10^{-3}	4.586×10^{-3}	3.380×10^{-3}
	Max Power (MW)	2.0	1.5	1.8	2.5
	Max PV Power (MW)	1			
	Load Demand (MW)	$1-4$			
	EV Load (kW)	500			
MG2	α	1.5×10^{-5}	2.5×10^{-5}	2×10^{-5}	
	β	1.8×10^{-3}	2.4×10^{-3}	4×10^{-3}	
	γ	0.120	0.080	0.075	
	a	2.543×10^{-3}	4.258×10^{-3}	5.426×10^{-3}	
	b	-6.047×10^{-3}	-5.094×10^{-3}	-3.550×10^{-3}	
	c	5.638×10^{-3}	4.586×10^{-3}	3.380×10^{-3}	
	Max Power (MW)	1.6	1.5	1.9	
	Max PV Power (MW)	1			
	Load Demand (MW)	$1-4$			
	EV Load (kW)	400			

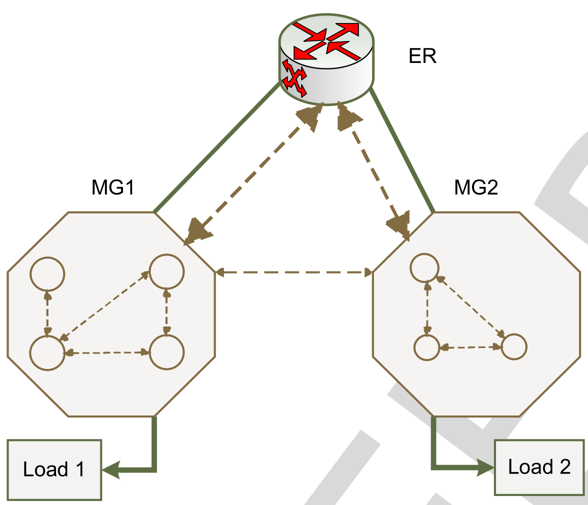

Fig. 3. Communication among DGs and power exchange between MGs via energy router.

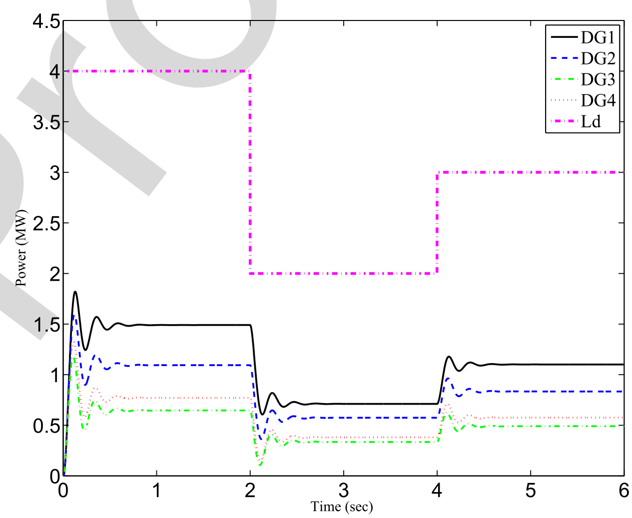

Fig. 4. Optimal power generation based on integral type optimized control.

are configured with constant values as $k_{p_i} = 2000$, $\tilde{k}_{p_i} = 400$, $k_{\phi_i} = 20$, $\forall i$, and $k_\lambda = 30$.

1) Performance Analysis for DPC: In this case, the performance of integrator-based controller is compared with the proposed DPC-based optimized power generation for ED. For this scenario, the parameter δ is set equal to one-half of the load demand. This setting restricts the maximum generated power difference between any pair of generators not more than half of the load demand. The performance of integral control for ED is shown in Fig. 4. It can be observed from Fig. 4 that the system response exhibits poor transient performance. There is high overshoot at the beginning as system tries to adjust the power from different generation units. It takes approximately 0.60 s to reach steady state. Transients are introduced at 2 and 4 s time instances, by exposing the system to step changes in load demands i.e., from $\frac{1}{2}L_d$ to Ld and then to $\frac{3}{4}L_d$, respectively. For these step changes in the load demand, poor transient performance is observed again. Same load transient scenario is applied to optimized DPC and the response is shown in Fig. 5. Values for DPC gains used for this case are tabulated in Table III. From Fig. 5, a significant improvement is observed in transient performance and system settles in less than 0.2 s. In addition, overshoot is also reduced considerably, as shown in Fig. 5. Q4

2) Effect of PV Power Variation: To further explore the transient response of proposed solution, PV power variation is taken into account. A step change in PV power from its nominal generation of 1.5–1.2 MW is tested. The DGs power generation due to PV power variation at 1–2 s interval is adjusted. Load L_d is reduced at 3 s instance from 4 to 3 MW and corresponding DGs power generation is reduced, resulting in reduced thermal generation cost and emission cost. Fig. 6 clearly shows a superior performance of the optimized control under load and source PV power variation, while resulting in improved dynamic performance.

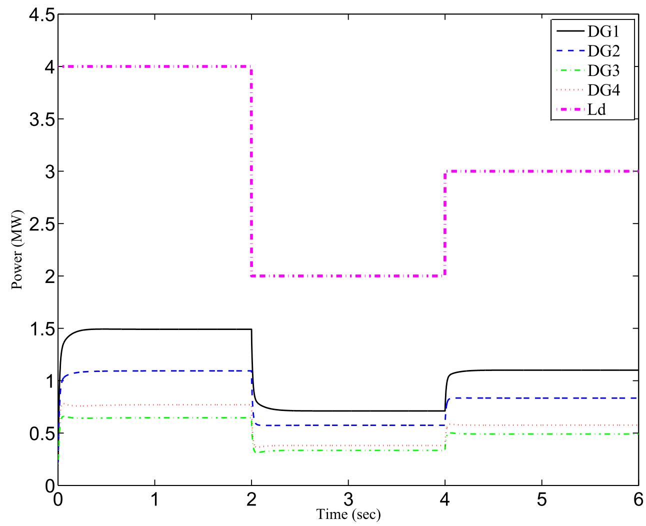

Fig. 5. Optimal power generation based on DPC type optimized control.

TABLE III
GAIN VALUES FOR DPC

Parameter	DG1	DG2	DG3	DG4
$k_3^{(i)}$	0.006	.006	0.008	0.008
$k_2^{(i)}$	.01	.01	.01	.01
$k_1^{(i)}$	.1	.18	.2	.06

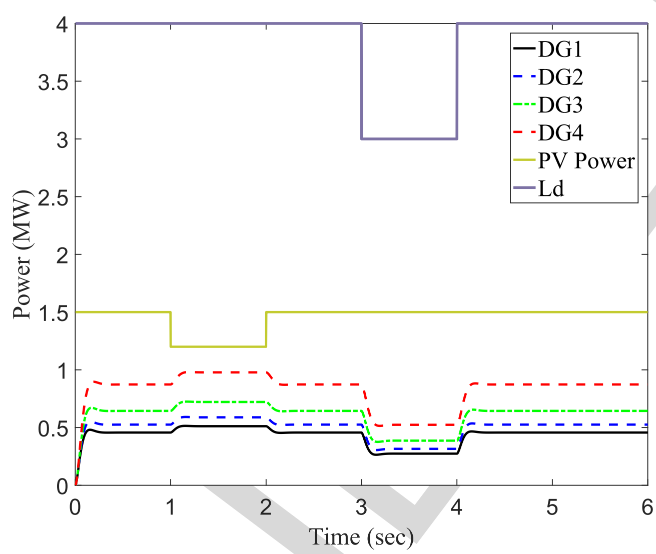

Fig. 6. Effect of PV power intermittency and load variation on DG power output.

3) Effect of Time Varying EV Load on Integral and Optimized Controller: In this case, the measured data from [28] is used to model load of an EV charging and discharging for a Nissan Leaf EV, having 50 kW normal charging load to get further insight on the transient behavior of proposed solution. The results are shown in Fig. 7(a) and (b). When the charging load of 5 MW for a fleet of Nissan Leaf EVs is applied for up to 1.5 s, the generators share this load. A step change in load is introduced at 1.5 s. Performance of integral control is compared with that of proposed DPC. As depicted in Fig. 7, integral controller has poor transient performance compared to DPC. After 2 s, the EV batteries are discharged, the load demand on generators due to EV's batteries is also adjusted and followed closely by the DGs. From these results, it is obvious that DPC has superior dynamic performance compared to integral controller and distributed optimized control is adapting time varying load conditions. In a different scenario with the presence of time varying EV charging load, DG power adjustment, emission cost, and generation cost variations are studied. In this case, EV charging load, LEV $= 50$ kW is varied at $t = 2$ s for a single Nissan Leaf EV along with normal load of $L_d = 500$ kW applied to MG. Fig. 8(a)–(c) shows the results for DG power adjustment, emission cost, and generation cost of the generators. It is obvious from these results that distributed optimization is working and dynamics in each case is following time varying EV load.

B. MMG With Energy Routing

1) Power Sharing Between Two MGs: Two MGs, MG1 and MG2 have been considered in this case. The connectivity between MG1 and MG2 having four and three DGs, respectively, is illustrated in Fig. 3. For given connectivity among DGs in MG1 the corresponding Laplacian matrix M_1 is given in (27) and for that of MG2 (M_2) is

$$M_2 = \begin{bmatrix} 2 & -1 & -1 \\ -1 & 2 & -1 \\ -1 & -1 & 2 \end{bmatrix}. \tag{28}$$

Various parameters such as generation and emission cost coefficients, power limits of various DGs, PV power and EV loads are provided in Table II. Each MG has a PV power source with maximum power rating of 1 MW. Simulation results are provided in Fig. 9. MG1 is supplying a load of 4 MW when there is an additional 1 MW demand from 10 to 30 s as shown in Fig. 9(a). MG1 can meet this load demand because its DGs can provide additional power. Some of this power will be provided by DGs of MG1 but not all due to its increased generation cost. At this instance energy router allows power flow from MG2 to MG1, due to lower generation cost at MG2 (see MG2 parameters in Table II). MG2 DGs will generate additional power to partly meet the load demand of MG1 as shown in Fig. 9(b). As a result, power flows from MG2 to MG1 as shown in Fig. 9(c).

2) Energy Output/Demand and Comparison With [17]: In this case, we compare performance of our proposed control with Fig. 5(a) from [17]. The basis of comparison is with (31) in [17], which is quadratically augmented Lagrangian function. A distributed consensus based ADMM algorithm is developed by authors and results are obtained for optimal powers [17]. In our case, the choice of Lagrangian function is given by (16). We consider two MGs (energy bodies in [17]) MG1 with four generators (participants in [17]) and MG2 with three generators (participants in [17]). The rating of the generators are similar to those used by [17]. Results of this comparison are shown in Fig. 10. Fig. 10(a) and (b) corresponds to Fig. 5(a) in [17]. It is clear from Fig. 10(a) that dynamic performance of ADMM

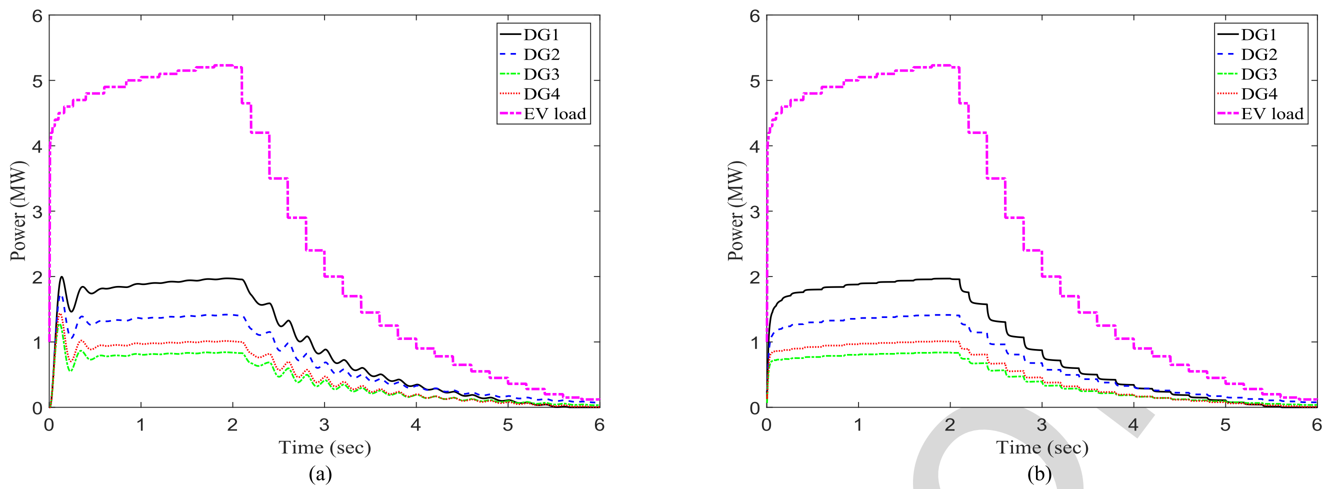

Fig. 7. (a) Integral controller performance with time varying EV load. (b) Optimized controller performance with time varying EV load.

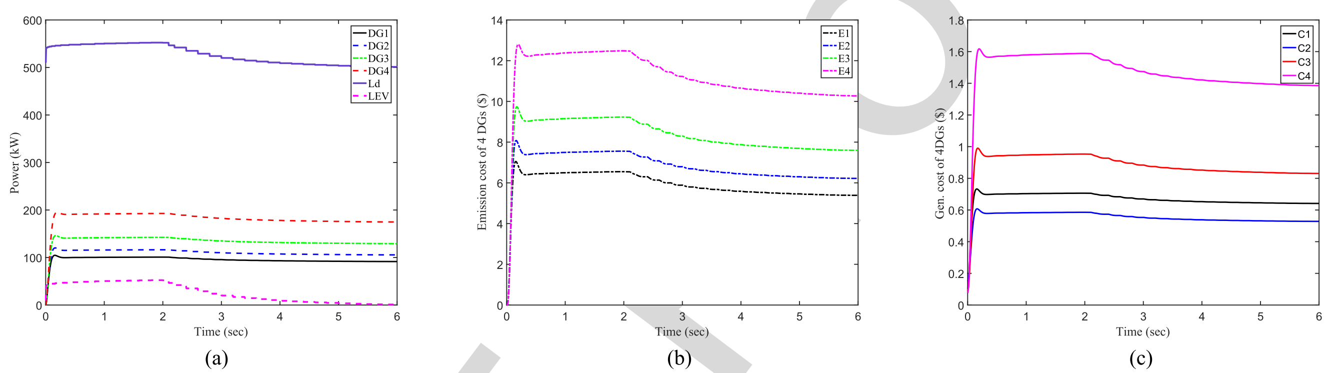

Fig. 8. (a) DG power adaptation with time varying EV load. (b) Emission cost with time varying EV load. (c) Generation cost with time varying EV load.

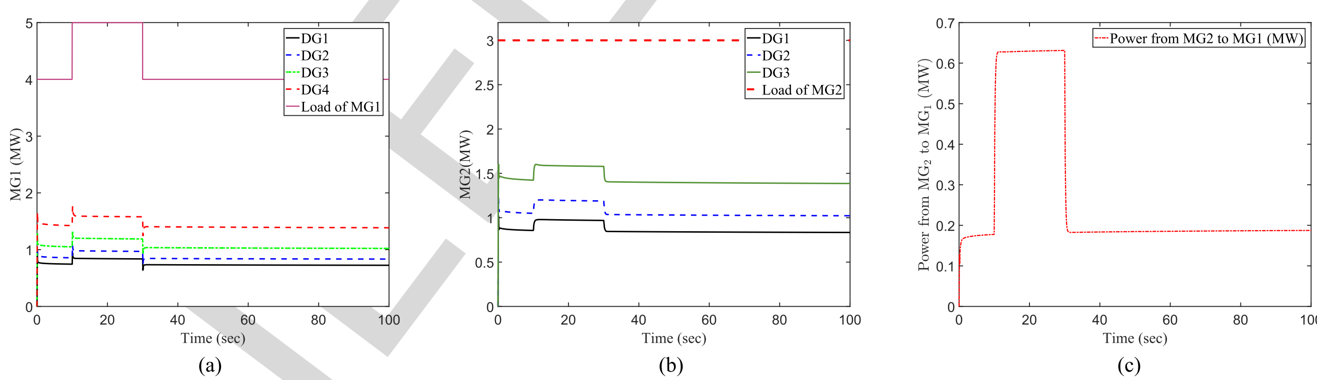

Fig. 9. Power sharing between two MGs with increased load demand in MG1(a) MG1 DG powers and load. (b) MG2 DG powers and load. (c) Power from MG2 to MG1.

is not good and there are power oscillations around the optimal point. We can also observe this in Fig. 5(a) in [17] that there is high overshoot before reaching optimal value. To remove these oscillations, the parameters are tuned further and results are provided in Fig. 10(b). Consensus among generators is achieved but no of iterations to achieve this are increased and there is high overshoot similar to Fig. 5(a) in [17]. Result for proposed control is given in Fig. 10(c), which shows clear improvement in dynamic performance and objective of consensus is also achieved in fewer iterations. Q5

3) Plug and Play Capability Verification and Comparison With [17]: To verify Plug-and-Play (PnP) capabilities, DG1 and DG3 in MG1 are intentionally disconnected at $t = 16.67$ s and $t = 50$ s (their communication links are also interrupted), until

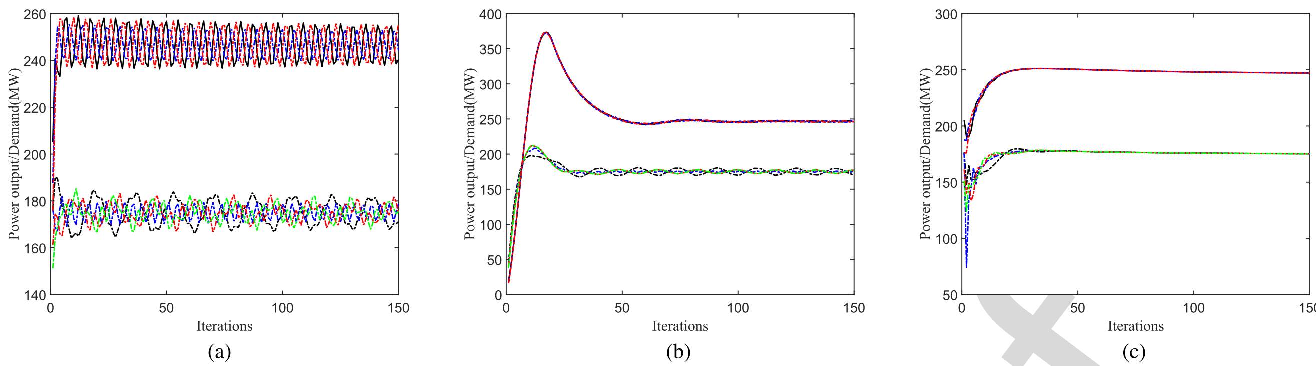

Fig. 10. Comparison with [17] power output/demand (a) DG powers using' in [17]. (b) DG powers using ADMM in [17] with better tuning. (c) DG powers using proposed DPC control.

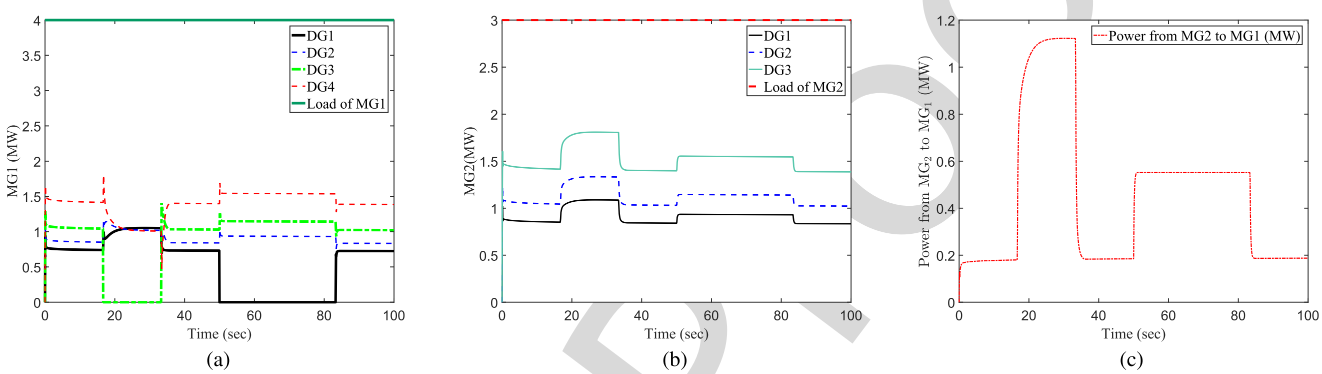

Fig. 11. PnP capability verification and comparison with [17]. (a) MG1 DG powers and load with DG1 and DG3 plug-out/plug-in. (b) MG2 DG powers and load. (c) Power from MG2 to MG1.

$t = 33.34$ s and $t = 83.34$ s, when these DGs join back MG1 again. Fig. 11 depicts the performance of the proposed controller for this scenario. MG1 supplies its normal load of 4 MW and MG2 supplies its normal load of 3 MW. When DG3 is disconnected at $t = 16.67$ s, MG1's DGs can supply only 3 MW as shown in Fig. 11(a). MG2 DGs increase their power production between $t = 16.67$ s and $t = 33.34$ s as shown in Fig. 11(b) and about 1 MW is supplied to MG1. 1 MW is routed from MG2 to MG1 as shown in Fig. 11(c). A similar scenario is shown when DG1 is plugged out at $t = 50$ s and then plugged in at $t = 83.34$ s. MG2 DGs increase their power production between $t = 50$ s and $t = 83.34$ s. This PnP feature clearly indicates that, once DG1 or DG3 leaves MG1, other DGs in MG2 increase their supplied active powers proportional to their rated values meeting total load demand. Comparing this PnP feature with Fig. 7(a) of [17], it is obvious that there are transients in Fig. 7(a) at plug-out/plug-in instants in [17]. However, proposed solution has smooth power transitions when DGs are plug-out/plug-in and shows the better dynamic performance of our control.

VI. Conclusion

The problem of optimized control for DG and their ED is considered for a single as well as MMG scenario. Specifically, as a first step augmented Lagrangian approach along with MAS model, is used to design a DPC, which provides improved transient performance for single MG scenario. The system model integrates renewable sources, such as PV as well as EVs, to further study the performance improvement provided by DPC. The proposed solution for single MG is extended to MMG by introducing energy router concept. The performance evaluation results also show the performance improvement during load (e.g., EV) as well as source (e.g., PV) transients. The optimal power flow in case of an MMG is achieved using distributed optimization. We anticipate that the scaling of proposed MMG architecture will lead to Energy-Internet.

References

[1] K. Boroojeni, M. H. Amini, A. Nejadpak, T. Dragievi, S. S. Iyengar, and F. Blaabjerg, "A novel cloud-based platform for implementation of oblivious power routing for clusters of microgrids," *IEEE Access*, vol. 5, pp. 607–619, 2017.

[2] E. J. Harmon, U. Ozgur, M. H. Cintuglu, R. de Azevedo, K. Akkaya, and O. A. Mohammed, "The internet of microgrids: A cloud based framework for wide-area networked microgrids," *IEEE Trans. Ind. Inf.*, vol. 14, no. 3, pp. 1262–1274, Mar. 2018.

[3] G. Bedi, G. K. Venayagamoorthy, R. Singh, R. Brooks, and K. C. Wang, "Review of internet of things (IoT) in electric power and energy systems," *IEEE Int. Things J.*, vol. 5, no. 2, pp. 847–870, Apr. 2018.

[4] Y. Han, K. Zhang, H. Li, E. A. A. Coelho, and J. M. Guerrero, "Mas-based distributed coordinated control and optimization in microgrid and microgrid clusters: A comprehensive overview," *IEEE Trans. Power Electron.*, vol. 33, no. 8, pp. 6488–6508, Aug. 2018.

[5] L. Sigrist, E. Lobato, F. M. Echavarren, I. Egido, and L. Rouco, *Island Power Syst*. Boca Raton, FL, USA: CRC press, 2016.

[6] T. Ding and Z. Bie, "Parallel augmented Lagrangian relaxation for dynamic economic dispatch using diagonal quadratic approximation method," *IEEE Trans. Power Syst.*, vol. 32, no. 2, pp. 1115–1126, Mar. 2017.

[7] Y. Xu and Z. Li, "Distributed optimal resource management based on the consensus algorithm in a microgrid," *IEEE Trans. Ind. Electron.*, vol. 62, no. 4, pp. 2584–2592, Apr. 2015.

[8] A. Cherukuri and J. Cortés, "Distributed generator coordination for initialization and anytime optimization in economic dispatch," *IEEE Trans. Control Netw. Syst.*, vol. 2, no. 3, pp. 226–237, Sep. 2015.

[9] V. Loia and A. Vaccaro, "Decentralized economic dispatch in smart grids by self-organizing dynamic agents," *IEEE Trans. Syst., Man, Cybern.: Syst.*, vol. 44, no. 4, pp. 397–408, Apr. 2014.

[10] Y. A. Abass, A. T. Al-Awami, and T. Jamal, "Integrating automatic generation control and economic dispatch for microgrid real-time optimization," in *Proc. IEEE Power Energy Soc. General Meet*, 2016, pp. 1–5.

[11] J. Ahmad, M. Tahir, and S. K. Mazumder, "Dynamic economic dispatch and transient control of distributed generators in a microgrid," *IEEE Syst. J.*, 2018, to be published. Q6

[12] Y. Z. Li *et al.*, "Optimal operation of multi-microgrids via cooperative energy and reserve scheduling," *IEEE Trans. Ind. Inform.*, vol. 14, no. 8, pp. 3459–3468, Aug. 2018.

[13] M. J. Hossain, M. A. Mahmud, F. Milano, S. Bacha, and A. Hably, "Design of robust distributed control for interconnected microgrids," *IEEE Trans. Smart Grid*, vol. 7, no. 6, pp. 2724–2735, Nov. 2016.

[14] N. Cai, N. T. T. Nga, and J. Mitra, "Economic dispatch in microgrids using multi-agent system," in *Proc. North Amer. Power Sympo.*, 2012, pp. 1–5.

[15] A. Jubril, O. Olaniyan, O. Komolafe, and P. Ogunbona, "Economic-emission dispatch problem: A semi-definite programming approach," *Appl. Energy*, vol. 134, pp. 446–455, 2014.

[16] H. Kanchev, F. Colas, V. Lazarov, and B. Francois, "Emission reduction and economical optimization of an urban microgrid operation including dispatched PV-based active generators," *IEEE Trans. Sustain. Energy*, vol. 5, no. 4, pp. 1397–1405, Oct. 2014.

[17] H. Zhang, Y. Li, D. W. Gao, and J. Zhou, "Distributed optimal energy management for energy internet," *IEEE Trans. Ind. Inform.*, vol. 13, no. 6, pp. 3081–3097, Dec. 2017.

[18] Y. Zheng, Y. Song, D. J. Hill, and Y. Zhang, "Multiagent system based microgrid energy management via asynchronous consensus ADMM," *IEEE Trans. Energy Convers.*, vol. 33, no. 2, pp. 886–888, Jun. 2018.

[19] J. Miao, N. Zhang, C. Kang, J. Wang, Y. Wang, and Q. Xia, "Steady-state power flow model of energy router embedded ac network and its application in optimizing power system operation," *IEEE Trans. Smart Grid*, vol. 9, no. 5, pp. 4828–4837, Sep. 2018.

[20] S. Hambridge, A. Q. Huang, and R. Yu, "Solid state transformer (SST) as an energy router: Economic dispatch based energy routing strategy," in *Proc. IEEE Energy Convers. Congr. Expo.*, 2015, pp. 2355–2360.

[21] R. Wang, J. Wu, Z. Qian, Z. Lin, and X. He, "A graph theory based energy routing algorithm in energy local area network," *IEEE Trans. Ind. Inform.*, vol. 13, no. 6, pp. 3275–3285, Dec. 2017.

[22] D. Feijer and F. Paganini, "Stability of primaldual gradient dynamics and applications to network optimization," *Automatica*, vol. 46, no. 12, pp. 1974–1981, 2010.

[23] S. Poslad, "Specifying protocols for multi-agent systems interaction," *ACM Trans. Auton. Adapt. Syst.*, vol. 2, no. 4, Nov. 2007. [Online]. Available: http://doi.acm.org/10.1145/1293731.1293735

[24] S. Boyd and L. Vandenberghe, *Convex Optimization*. Cambridge, U.K.: Cambridge Univ. Press, 2004.

[25] D. Feijer and F. Paganini, "Stability of primal-dual gradient dynamics and applications to network optimization," *Automatica*, vol. 46, no. 12, pp. 1974–1981, 2010.

[26] M. Tahir and S. K. Mazumder, "Self-triggered communication enabled control of distributed generation in microgrids," *IEEE Trans. Ind. Inform.*, vol. 11, no. 2, pp. 441–449, Apr. 2015.

[27] Y. Xu, W. Zhang, and W. Liu, "Distributed dynamic programming-based approach for economic dispatch in smart grids," *IEEE Trans. Ind. Inform.*, vol. 11, no. 1, pp. 166–175, Feb. 2015.

[28] R. C. Leou, J. H. Teng, and C. L. Su, "Modelling and verifying the load behaviour of electric vehicle charging stations based on field measurements," *IET Gener., Transmiss. Distrib.*, vol. 9, no. 11, pp. 1112–1119, 2015.

Jameel Ahmad received the B.Sc. degree in electrical engineering from University of Engineering and Technology, Peshawar, Peshawar, Pakistan, in 1993, the M.S. degree in systems engineering from Quaide Azam University, Islamabad, Pakistan, in 1996, and the M.Sc. degree in electrical engineering from the University of Southern California, Los Angeles, CA, USA, in 2005. He is currently working toward the Ph.D. degree in electrical engineering at the University of Engineering and Technology, Lahore, Lahore, Pakistan.

From 2007 to 2010, he was with the Qualcomm and Broadcom Corporation, San Diego, CA, USA. Since 2010, he has been an Assistant Professor with the Department of Electrical Engineering, School of Engineering, University of Management and Technology, Lahore, Pakistan. His research interests include control and optimization of smart microgrids for energy internet.

Prof. Ahmad is a reviewer of numerous IEEE journals and conferences.

Muhammad Tahir (M'02) received the Ph.D. degree in electrical and computer engineering from the University of Illinois at Chicago, Chicago, IL, USA, in 2008.

He is currently a Professor with the Department of Electrical Engineering, University of Engineering and Technology, Lahore, Lahore, Pakistan. His research interests include wireless sensor networks, delay tolerant networks, distributed resource optimization for wireless networks, and real-time wireless multimedia networks. Further details about his current research activities can be found at www.uet.edu.pk/pp/ee/˜mtahir/

Sudip K. Mazumder (S'97–M'01–SM'03–F'16) received the Ph.D. degree in electrical and computer engineering from Virginia Tech, Blacksburg, VA, USA, in 2001.He is currently a Professor with the University of Illinois at Chicago, Chicago, IL, USA, since 2001, and is the President of NextWatt LLC since 2008. He has more than 25 years of professional experience and has held R&D and Design Positions in leading industrial organizations and has served as a Technical Consultant for several industries. He has authored or coauthored more than 210 refereed papers, delivered more than 90 keynote/plenary/distinguished invited presentations, and received about 50 sponsored research grants, since joining UIC.

Dr. Mazumder is a Distinguished Lecturer for IEEE Power Electronics Society (PELS) and a Chair for PELS Technical Committee on Sustainable Energy Systems. He is the new Editor-at-Large for the IEEE Transactions on Power Electronics (2019).